New Journal of Physics
The open access journal at the forefront of physics

Deutsche Physikalische Gesellschaft DPG
IOP Institute of Physics

Published in partnership with: Deutsche Physikalische Gesellschaft and the Institute of Physics

OPEN ACCESS

RECEIVED
15 June 2017

REVISED
18 September 2017

ACCEPTED FOR PUBLICATION
29 September 2017

PUBLISHED
30 November 2017

PAPER

Nonequilibrium dielectric noise in solids in the presence of modulation of electrical permittivity and spectral symmetry breaking under feedback

Dhiraj Sinha , Roland Bouffanais and Shao Ying Huang

Singapore University of Technology and Design, 8 Somapah Road, 487372, Singapore

E-mail: dhiraj_sinha@sutd.edu.sg

Keywords: dielectric, nonequilibrium, noise, fluctuation

Abstract

We present an analytical study on the generation of broadband electromagnetic noise in solids as a consequence of variations in the dielectric constant under the impact of polarization induced by nonequilibrium thermodynamic fluctuations. The analysis leads to a specific formulation of the fluctuation dissipation theorem in the context of dielectric materials having finite electrodynamic boundary conditions, which drive energy into the system, under feedback, during its under interaction with a heat bath. The ensuing spectral symmetry breaking of the broadband noise yields bursts of narrowband signals, which can potentially result in phase transitions and dielectric breakdown. This study sheds a new light on high temperature precision calorimetry, while also improving our understanding of unexpected breakdowns in devices like CMOS components, capacitors and batteries.

1. Introduction

Thermodynamic fluctuations are associated with the occurrence of noise in electronic devices, which is known as Nyquist–Johnson noise [1, 2]. Shot noise ensues from the discrete nature of electrons, thereby causing fluctuations around a mean value [3, 4]. Both Johnson and shot noises form the key component of Additive White Gaussian noise [5]. Despite intense developments in the field of miniaturization of electronic components, our basic understanding of electronic noise has not significantly changed over the past 90 years. However, other sources of noise—noise generated by thermoacoustic fluctuations in ultrasonic receiver circuits [6] and noise generated by capacitive components as a consequence of the polarization of dielectric material—have also been reported [7, 8]. As miniaturization of electronic devices has led to transistors with dielectric barriers between gate and drain-source channel going below 50 nm [9], the role of noise generated by dielectric materials may no longer be neglected and therefore requires further investigation. Dielectric noise also becomes important in radiofrequency systems, where dielectric materials are present in memory and logic devices [10] as well as filters [11]. Optical fibers are also made of dielectric materials and carry optical signals over long distances [12]. As the optical signal is launched in an optical fiber, a substrate of lithium niobate introduces a certain amount of phase shift in the optical signal depending on the input digital signal [13]. As a consequence, a study of dielectric material as an additional source of noise under thermodynamic fluctuations is timely and holds special importance given the practical implications in modern optoelectronic devices.

A minimalist model of noise generated by dielectric materials consists in equating the capacitive energy of a CMOS circuit with one half of the Boltzmann energy, thus leading to the expression of capacitive noise voltage as $V_{\mathrm{CN}} = \sqrt{k_{\mathrm{B}}T/C_T} = \sqrt{k_{\mathrm{B}}T/(\varepsilon C_a)}$ (see [7, 8]). Here, k_{B} is the Boltzmann constant, T is the temperature and C_T is the total capacitance which is equal to εC_a where $\varepsilon = \varepsilon_0\varepsilon_r$ and ε_0 is the permittivity of free space, ε_r is the medium's relative permittivity, and C_a is the capacitance of the system when the dielectric material is air. This simple formulation can be used to calculate the noise generated by finite values of capacitances in a circuit. To incorporate the effect of noise generated by nonequilibrium thermodynamic fluctuations, a new modeling framework is required. Here, we propose a formulation accounting for such nonequilibrium thermodynamic

fluctuations in the dielectric constant. In this framework, we show that at a given temperature, nonequilibrium thermal interactions can shift the position of charge centers leading to momentary polarization. This momentary polarization induces transient changes in the dielectric constant eventually generating additional noise in the system. Furthermore, our framework accounts for the energy feedback associated with the presence of finite boundary conditions, which induces spectral symmetry breaking of existing modes, eventually leading to noise enhancement.

2. Noise generated by thermodynamic fluctuations in a dielectric material

Atoms in a dielectric crystal are arranged in a regular lattice pattern. We consider that the charge cloud of each atom in the lattice is a sphere of radius R. When an electric field is applied, the charge cloud is momentarily distorted and is displaced by a distance x. Assuming Z to be the atomic number of the atom and e the elementary electronic charge, an electric charge with a value of $q = -Ze$ is present around the nucleus. An electric field E applied to the system leads to a net force expressed by [13]

$$(Ze)E = \frac{(Ze)^2}{4\pi\varepsilon_0}\frac{x}{R^3}, \tag{1}$$

where ε_0 is the permittivity of free space. The interaction of the atoms of the crystal with a heat bath induces a fluctuating force causing random vibrations of atoms of the lattice about their respective mean positions. Thus, the charge cloud can be distorted even in the absence of an external electric field (figure 1(a)). It leads to the induction of a fluctuating electric field having an instantaneous value $E(t)$ associated with a force field $F(t)$, generated as a consequence of thermodynamic fluctuations. The instantaneous displacement of the center of charge cloud in such a case is $x(t) = 4\pi\varepsilon_0 R^3 E(t)/Ze$ and the corresponding dipole moment can be expressed as

$$\mu_{\text{ind}}(t) = (Ze)x(t) = 4\pi\varepsilon_0 R^3 E(t) = \alpha_{\text{ind}} E(t). \tag{2}$$

This gives the expression of the polarizability constant (in C m^2 V^{-1}), $\alpha_{\text{ind}} = 4\pi\varepsilon_0 R^3$, since the polarization is defined as the electric dipole moment per unit volume [14]. Hence, with N atoms per unit volume, the average polarization can be expressed as

$$P(t) = N\alpha_{\text{ind}} E(t) = N4\pi\varepsilon_0 R^3 E(t). \tag{3}$$

Based on equation (3), it can be seen that atoms with a larger atomic radius are more easily polarized than those with smaller radii. The electric flux density at any instant of time is given by $D(t) = \varepsilon_0 E(t) + P(t)$. By using the relationship $D(t) = \varepsilon_0\varepsilon_r E(t)$ and equation (3), the dielectric constant can be expressed as,

$$\varepsilon_r = N\alpha_{\text{ind}}/\varepsilon_0 + 1 = 4\pi N R^3 + 1. \tag{4}$$

Equation (4) relates the induced polarization, dielectric constant and atomic radius. Any change in the value of R would result in a change in the value of the induced polarization as well the value of the dielectric constant. In order to simplify the physics of the problem, the orientational and ionic polarization have been assumed to be negligible along with the locally induced internal electric field in the given solid material.

Heat applied to a crystal induces a relative displacement of the nuclei in an atom around its mean position and a distortion of the electron cloud. Polarization induced by thermal nonequilibrium fluctuations yields effective fluctuations in the radius R of the charge cloud. It leads to a shift in the position of electron charge cloud away from the positively charged nucleus as illustrated in figure 1(a). The electron charge cloud and the nucleus are at different positions at different instants of time under thermodynamic fluctuations leading to an increase in the effective radius of the atom (figure 1(b)). As this process occurs over the entire crystal, an expansion of the charge cloud of a number of atoms can momentarily compress the electron charge cloud of some atoms (figure 1(c)) leading to random compressions and expansions of the effective atomic radius around some mean position, which can be modeled using a Gaussian function.

We consider a two-dimensional charge cloud distribution along the x- and y-axis where a coordinate point d along an angular orientation θ has coordinate values ($x = d\cos\theta$, $y = d\sin\theta$) along the two axes. An increase in the radius of the charge cloud can be expressed by a mathematical function $g(r, \theta)$ such that

$$[f_x(r, \theta)]^2 + [f_y(r, \theta)]^2 = [g(r, \theta)]^2, \tag{5}$$

where $f_x(r, \theta)$ and $f_y(r, \theta)$ are differential changes of the radius R of the electron cloud along the x- and the y-direction respectively. The expansion of the electron cloud at an angle of $\pi/4$ from the origin is symmetric along the x and y coordinates, hence, it can be assumed that $f_x(x) = f_y(y)$ and equation (5) can be written as

$$2[f_x(r, \theta)]^2 = 2[f_y(r, \theta)]^2 = 2[f_x(r, \theta)][f_y(r, \theta)] = [g(r, \theta)]^2. \tag{6}$$

We assume that the expansion of the charge cloud is constant for a given amount of heat absorption along a specific direction. When the absorbed heat is released by the system, it retains its initial shape. Thus, for a given

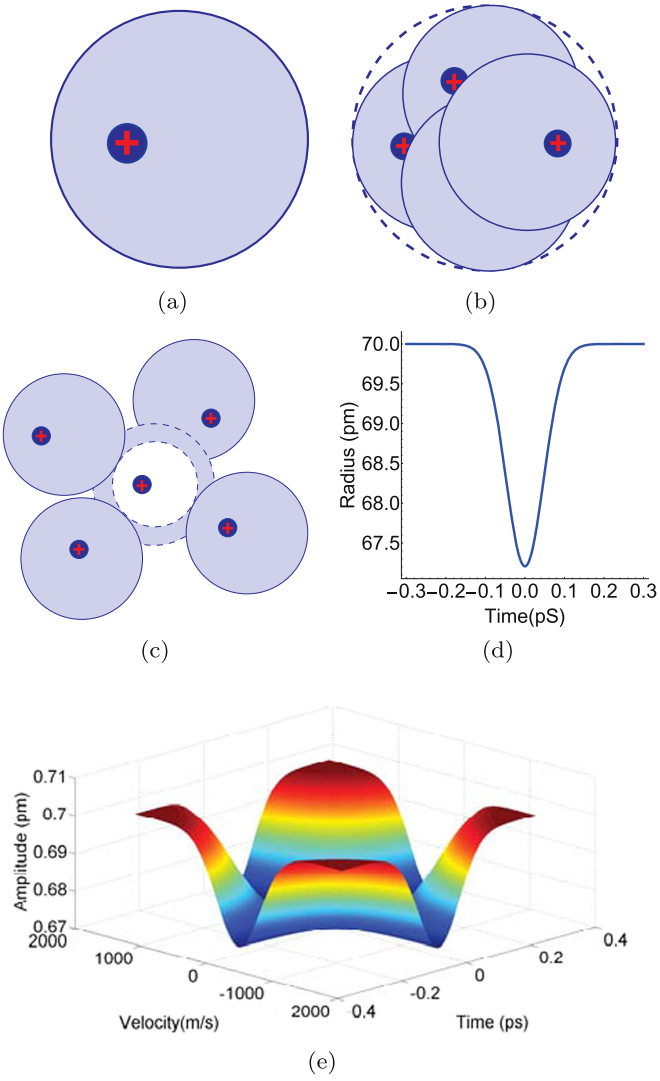

Figure 1. Shift in electron cloud around a nucleus and change in effective radius. (a) The electron cloud around the positively charged nucleus is shifted under nonequilibrium thermodynamic fluctuations. (b) The differential shift in the position of the electron cloud in space around the nucleus of a single atom under thermodynamic fluctuations can lead to a transient increase in its effective radius as a consequence of fluctuating positions of the charge cloud about its mean position with time represented by the dashed circle. (c) Shift in effective radius of atoms can also result in compression of charge clouds of a set of atoms around it leading to a decrease in the effective radius denoted by the dashed circles. (d) Reduction in effective radius of charge cloud under thermodynamic fluctuations can be modeled using a Gaussian function. The atomic radius is assumed to be $R = 70$ pm—atomic radius of carbon, which is assumed to contract by 10%. (e) Three-dimensional illustration of change of radius with variations in velocities along with time variations.

event associated with heat absorption, r and θ are constants. With a change in angular orientation, the values of r and θ will change. They would, however, remain constant for a specific configuration of heat absorption and change in the radius along any given angular orientation. Hence, $g(r, \theta)$ can be assumed to be constant for a specific case of thermal absorption by the charge cloud when $\theta = \pi/4$. Differentiating equation (6) with respect to θ yields

$$0 = f_x(r, \theta)\frac{\partial f_y(r, \theta)}{\partial y}\frac{\partial y}{\partial \theta} + f_y(r, \theta)\frac{\partial f_x(r, \theta)}{\partial x}\frac{\partial x}{\partial \theta}, \tag{7}$$

and subsequently to

$$0 = f_x(r, \theta)f_y'(r, \theta)r\cos\theta - f_y(r, \theta)f_x'(r, \theta)r\sin\theta. \tag{8}$$

Finally, we get

$$\frac{f_x'(r, \theta)}{xf_x(r, \theta)} = \frac{f_y'(r, \theta)}{yf(r, \theta)} = C, \tag{9}$$

where C is a constant, thus leading to

$$f_x(r,\theta) = Ae^{Cx^2/2},$$
$$f_y(r,\theta) = Ae^{Cy^2/2}.$$

Here, C must be negative to ensure that the functions remain bounded. In addition, C must have proper dimensions. Since the electron cloud radius R is the characteristic length scale of the problem, one can naturally write that $C = -C'/R^2$, where $C' = 1$ is dimensionless. Assuming spherical symmetry in the expansion of the charge cloud, the change of radius can be written as

$$g(r,\theta) = \sqrt{(f_x(r,\theta))^2 + (f_y(r,\theta))^2},$$
$$= \sqrt{(x_0 e^{-x^2/(2R^2)})^2 + (y_0 e^{-y^2/(2R^2)})^2}. \quad (10)$$

We obtain $g(r,\theta) = r_0 e^{-r^2/(4R^2)}$ by using the relation $x = y = r/\sqrt{2}$ and $x_0 = y_0 = r_0/\sqrt{2}$ for $\theta = \pi/4$, and $g(r,\theta) \ll R$. Because of spatial symmetry, this expression is valid for all values of θ. As the charge cloud expands, its rate of change with time can be written as $v_C = \mathrm{d}g/\mathrm{d}t = -rr_0 e^{-r^2/(2R^2)} v/(2R^2)$, where $v = \mathrm{d}r/\mathrm{d}t$ is related to the rate of expansion of the charge cloud. For the sake of simplicity, this motion can be considered as a simple linear ballistic process devoid of any diffusive character. Considering σ as the spectral width of the Gaussian pulse, and using $r = vt$, we can write the total radius of electron cloud under thermodynamic fluctuations as

$$R_T(t) = R + g(r,t) = R + \frac{r_0}{\sqrt{2\pi\sigma^2}} e^{-\frac{(vt)^2}{4\sigma^2R^2}}. \quad (11)$$

Here, σ is a dimensionless quantity characterizing the spectral width of the charge expansion. At the onset of the thermal expansion process, say at time $t = -t_0$, the Gaussian coefficient in equation (11) is close to zero as $t = -t_0 \ll 0$. Hence, the net effective radius of the charge cloud is R. The charge cloud expands from its initial equilibrium state and its radius reaches a maximum value at time $t = 0$, when the value of the Gaussian coefficient increases to its maximum value of one and the charge cloud has expanded to $r_0 + R$. At time $t = t_0 \gg 0$, the Gaussian coefficient is again zero leading to the initial value of radius of the charge cloud. Equation (11) can also be used to represent contraction of the radius by inserting a negative Gaussian term which is graphically illustrated in figure 1(d) for carbon with an atomic radius of $R = 70$ pm, which is assumed to have a maximum contraction of 10%, hence $r_0 = 7$ pm. Its density in graphite is assumed to be 9.4×10^{28} atoms m^{-3} [15]. The velocity of expansion of the radius is assumed to be equal to the phonon velocity in carbon [16]. The Gaussian dependence on velocity, as well as time of the effective radius, is illustrated in figure 1(e) considering a velocity variation from $+1450$ to -1450 m s^{-1}. The spectral width is assumed to be unity, while the phonon velocity in carbon nanotubes has been measured to be in the range of 1450 m s^{-1} [16]. Hence, the net value of the dielectric constant at time t can be written as

$$\varepsilon_r(t) = \frac{N\alpha_{\mathrm{ind}}(t)}{\varepsilon_0} + 1$$
$$= 4\pi N\left(R - \frac{r_0}{\sqrt{2\pi\sigma^2}} e^{-\frac{(vt)^2}{4\sigma^2R^2}}\right)^3 + 1. \quad (12)$$

The dependence of the dielectric constant—or equivalently the relative permittivity—on velocity and time is illustrated in figure 2(a), which shows a Gaussian profile over a period of 3 ps and a velocity in the range of -100 to $+100$ m s^{-1}. The slope of the Gaussian curve undergoes a sudden change with an increase in velocity as shown in figure 2(b), where the velocity variation is in the range of -2000 to $+2000$ m s^{-1}, which correspond to the velocity of phonon modes in solids, over the same period of time. Equating the Boltzmann energy to the capacitive energy of a capacitor of capacitance C_a, we get the fluctuation noise voltage as

$$V_{\mathrm{FN}}(t) = \sqrt{\frac{k_B T}{C_a}}\left[4\pi N\left(R - \frac{r_0}{\sqrt{2\pi\sigma^2}} e^{-\frac{(vt)^2}{4\sigma^2R^2}}\right)^3 + 1\right]^{-1/2}. \quad (13)$$

This is essentially a Gaussian function, which is graphically illustrated in figure 3(a) over a period of 3 ps. Equation (13) can be written in a simplified form as

$$V_{\mathrm{FN}}(t) = \sqrt{\frac{k_B T}{C_a}}\left[1 - 2\pi NR^3\left(1 - \frac{3r_0}{R\sqrt{2\pi\sigma^2}} e^{-\frac{(vt)^2}{4\sigma^2R^2}}\right)\right], \quad (14)$$

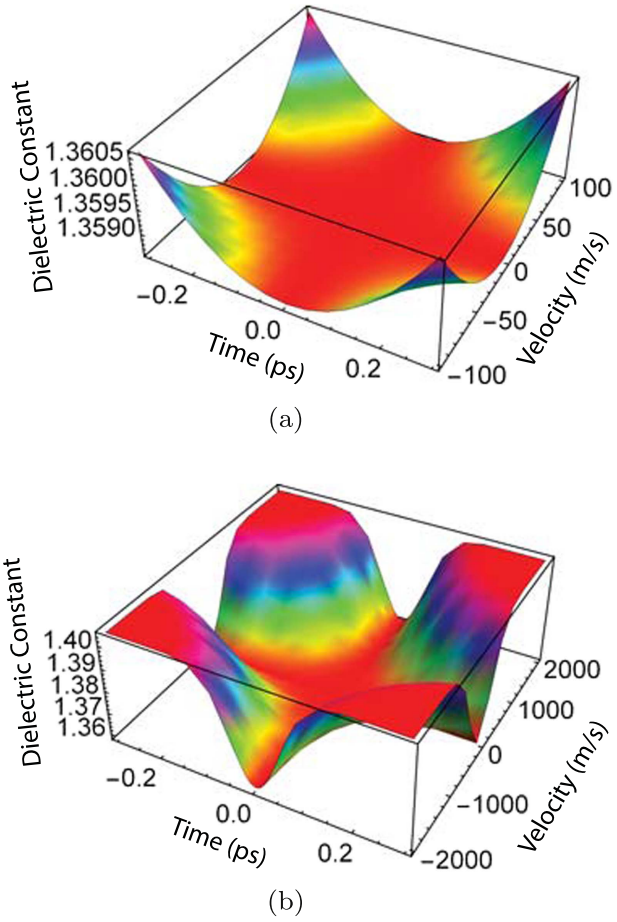

Figure 2. Change of relative permittivity with velocity of the charge cloud. (a) As the electron cloud contracts, the permittivity increases demonstrating a Gaussian profile which is symmetrically dependent on velocity as well as time. (b) An increase in velocity of the charge cloud decreases the spectral density of the Gaussian profile of permittivity value.

which can be further expanded and simplified as

$$V_{\mathrm{FN}}(t) = \alpha(1 - \beta + \chi \mathrm{e}^{-\xi t^2}), \tag{15}$$

where $\alpha = \sqrt{k_{\mathrm{B}} T / C_a}$, $\beta = 2\pi N R^3$, $\chi = 6\pi N \eta_0 R^2 / \sqrt{2\pi\sigma^2}$ and $\xi = v^2/(4\sigma^2 R^2)$. The Laplace transform of equation (15)—the thermodynamic response to an impulse input—is expressed as

$$V_{\mathrm{out}}(s) = \alpha\left[\frac{1}{s} - \frac{\beta}{s} + \frac{\chi}{2\sqrt{\xi}} \mathrm{e}^{s^2/4\xi}\sqrt{\pi}\ \mathrm{erfc}\left(\frac{s}{2\sqrt{\xi}}\right)\right]. \tag{16}$$

Its graphical illustration in figure 3(b) shows an exponential decay with an increase in frequency indicating thermodynamic stability of the system at relatively higher frequencies. The expansion of radius of an atom under thermodynamic fluctuations lasts in the range of picoseconds as illustrated in figure 1(d). The noise generated when the system is subjected to external excitation frequencies in the range of 1–10 THz is between 0.2 and 0.12 femtovolts, which is lower than Johnson noise. However, noise in a dielectric material increases asymptotically at excitation frequencies in the range of kHz as shown in figure 3(b), where it is in the range of μV. In a given dielectric material under thermodynamic fluctuations, capacitance is the critical determinant of noise and the noise increases in a hyperbolic manner with an increase in capacitance as represented by figure 3(c), where noise voltage is in the range of 6 μV at a capacitance of 0.1 nF. The capacitance is varied from 1 attofarad (corresponding to zero along the capacitance axis) to 10 femtofarad with a frequency variation from 0 to 1 kHz. The pattern of noise generation shows a hyperbolic dependence on capacitance as well as frequency as illustrated in figure 3(d).

The net change in effective radius with temperature would lead to some finite changes in the value of the dielectric constant. Specifically, the dependence of the dielectric constant with temperature can be expressed as

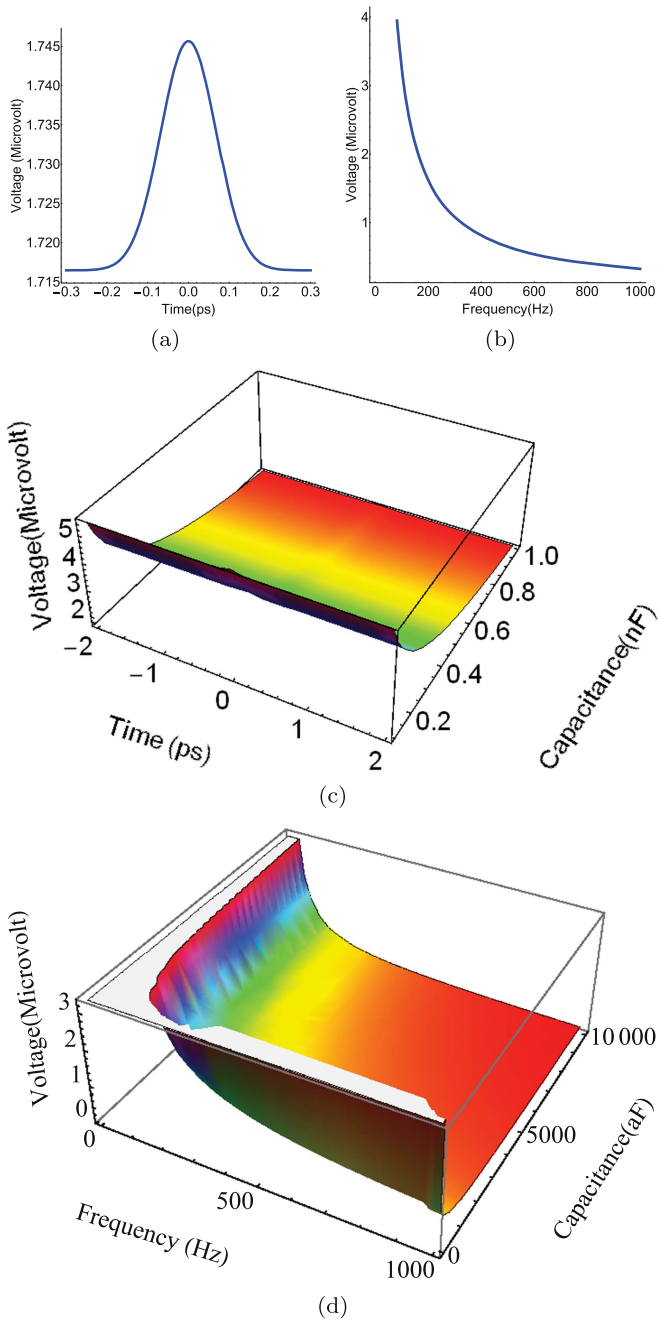

Figure 3. Noise generation under thermodynamic fluctuations. (a) Gaussian profile of noise voltage generation under thermodynamic fluctuations. (b) Frequency response of noise signal in a dielectric material under impulse response. The decaying curve represents stability which is a characteristic of electrodynamic homogeneity. (c) The overall capacitance is a dominant determinant of noise and it shows a hyperbolic increase with a reduction in capacitance. (d) The noise level shows a hyperbolic increase with a reduction in capacitance and frequency.

$$\frac{\partial \varepsilon_r(t)}{\partial T} = 12\pi N\left(\frac{r_0}{\sqrt{2\pi\sigma^2}}e^{-\frac{(vt)^2}{4\sigma^2R^2}} + R\right)^2 \left[\frac{r_0}{\sqrt{2\pi\sigma^2}}e^{-\frac{(vt)^2}{4\sigma^2R^2}}\left(\frac{1}{4\sigma^2R^2}\frac{\partial(vt)}{\partial T}\right)\right]. \quad (17)$$

3. Comparison with Johnson noise

The Johnson noise in a circuit of resistance R at a temperature T over a frequency band Δf is expressed as $V_{\mathrm{NR}} = \sqrt{4k_{\mathrm{B}}R_R T\Delta f}$ [1, 2]. At room temperature (300 K), the Johnson noise over a frequency band of 4 MHz is 1.95 μV. The noise generated by a capacitor of capacitance 1 nF is of the order of 2 μV, which is similar in terms

of orders of magnitude to the Johnson noise in a resistor. In order to evaluate the exact value of the noise generated by such fluctuations in the relative permittivity, an evaluation of the net change in radius at the atomic level is not needed. Indeed, the variations of the permittivity with temperature is an empirically observed quantity which can play an important role in noise calculation. Using the relationship for capacitive noise voltage, and considering the variation of permittivity with temperature, we get

$$\frac{\partial V_{\mathrm{CN}}}{\partial T} = \frac{1}{2}\sqrt{\frac{k_{\mathrm{B}}T}{C_a}}\left(\frac{1}{\varepsilon}\right)^{3/2}\frac{\partial \varepsilon}{\partial T} = \frac{1}{2}V_{\mathrm{CN}}\left(\frac{1}{\varepsilon}\right)^{3/2}\frac{\partial \varepsilon}{\partial T}. \tag{18}$$

For a material like lithium-niobate with a dielectric constant of 25, its value changes by 0.01 for every unit change in temperature up to 200 K [17]. Considering its dielectric constant to be 25, the net fluctuation in the capacitive noise is of the order of 5×10^{-5} [18]. Such noise levels can remain insignificant under normal conditions. However, the value of the dielectric constant rises sharply above 600 K and the associated fluctuations can drastically change the noise values under such cases. For example, if the dielectric constant is 25 and it changes by 5 units for every rise in temperature above 600 K, the net noise contribution would be 2.8% of the total capacitive noise. This is still a low figure, however, for sensors operating at extreme temperature conditions, the overall contribution from all electronic devices can become significant, particularly when changes in dielectric constant are severe. Today, there are gas sensors operating at temperatures above 673 K and slowly, the technology is shifting towards CMOS based sensors for such applications [19]. Fiber grating based sensors for such high temperature measurements have also been developed at around 823 K [20]. A careful analysis of noise induced by dielectric fluctuations in such sensors operating under extreme conditions could open new insights towards precision measurements.

4. Fluctuation dissipation theorem under feedback and mode enhancement

The mathematical expression for the Nyquist–Johnson noise leads to the fluctuation dissipation theorem, which states that noise spectrum generated under thermodynamic fluctuations results in dissipation and is expressed as $P_N = k_{\mathrm{B}}T\Delta f$ [1, 2]. It is worth adding that the spectral power density of the noise signal is independent of frequencies. As already mentioned, in the context of dielectric materials interacting with a heat bath, thermal fluctuations lead to transient electronic polarization, which modulates the radius of electron cloud leading to voltage and current generation. As the current is injected into the heat bath, the energy is dissipated, thus increasing the level of thermodynamic fluctuations which is again fed back into the dielectric material as illustrated in figure 4(a).

The dielectric material can be considered to be an inductor–capacitor circuit element in which the voltage induced by the thermodynamic fluctuation is transformed into current whose Joule dissipation modulates the intensity of the heat bath, which in turn, leads to a transient increase in the energy being transferred back to the system as thermodynamic fluctuations (figure 4(b)). The heat bath, at a physical level can be represented as the resistive component of the dielectric crystal, which is responsible for dissipation as well as thermodynamic fluctuations. However, the fluctuating thermodynamic energy of a particular dielectric crystal also gets coupled to other crystals in its proximity or to the open circuit boundary conditions. It happens because a crystal is not an infinitely long homogeneous piece of material immersed in a heat bath. Its finite dimensions as well as electrodynamic inhomogeneity imply that a part of the energy is fed back to it as the propagating modes encounter a discontinuity. This is depicted in figure 4(c), where a given crystal (C) exchanges energy with a heat bath. However, the crystal (C) is also coupled to other crystals in its vicinity or with its own finite boundaries which results in feeding the energy back to itself.

The second-order equation of a dielectric crystal can be written as [21]

$$L\frac{\mathrm{d}^2q}{\mathrm{d}t^2} + R\frac{\mathrm{d}q}{\mathrm{d}t} + \frac{q}{C_a} = V_{\mathrm{in}} + V_{\mathrm{FB}}, \tag{19}$$

where L is the inductance, R the resistance and C_a the capacitance of the crystal, V_{in} is the voltage induced from the heat bath into the crystal and V_{FB} is voltage fed back into the crystal directly as a consequence of the electrodynamic inhomogeneity or open boundary conditions of the system. The feedback voltage is expressed as V_{FB}

$$V_{\mathrm{FB}} = L^F\frac{\mathrm{d}^2q}{\mathrm{d}t^2} + R^F\frac{\mathrm{d}q}{\mathrm{d}t} + \frac{q}{C^F}, \tag{20}$$

with L^F the inductance, R^F the resistance and C^F the capacitance of the dielectric crystal driving the feedback voltage mechanism. Taking the Laplace transform of equations (19) and (20) and substituting the value of V_{FB}, we get

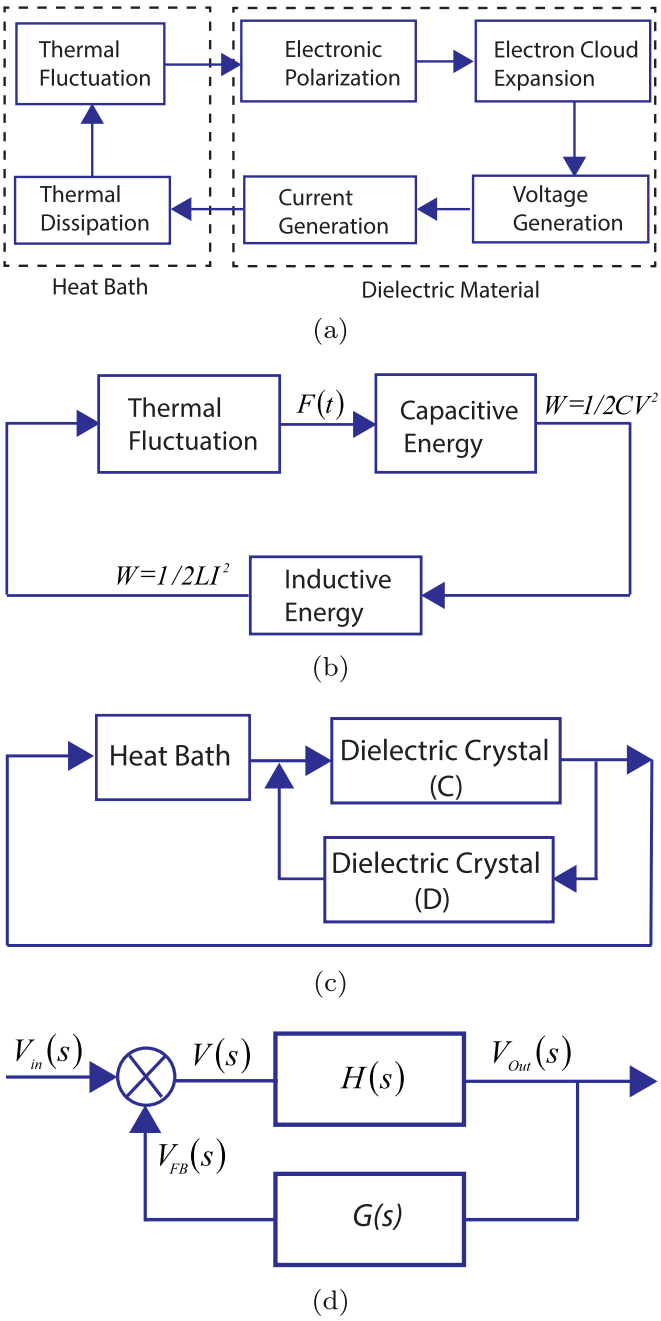

Figure 4. Energy enhancement under feedback. (a) Thermodynamic fluctuations from a heat bath get coupled to a dielectric material resulting in transient electronic polarization leading to electron cloud expansion that generates voltage and current. The current is eventually dissipated as heat which is fed to the heat bath. (b) The energy can oscillate between capacitive and inductive components of a dielectric material leading to some specific resonant modes. (c) A dielectric crystal (C) interacting with a heat bath transfers and receives energy from it. The dielectric crystal (C) has got structural asymmetries, for example, it has finite boundary conditions which results in feedback of energy. This aspect of the crystal can be considered as a distinct dielectric crystal (D) which actuates the feedback process. (d) Feedback can result in signal enhancement depending on the nature of the inhomogeneity which can trap energy. Here, the voltage $V(s)$ representing the spectral distribution of noise voltage is equal to $V_{\rm in}(s)$ at time $t = 0$. The output signal $V_{\rm out}(s)$ is generated as a consequence of its interaction with the system's impulse response which is fed back to the input as $V_{\rm FB}(s)$ where it is added to the noise input signal $V_{\rm in}(s)$.

$$(s^2 + 2s\omega_k\zeta + \omega^2)q = V_{\rm in}(s) - (s^2 + 2s\omega_F\zeta_F + \omega^2)q. \tag{21}$$

Here, $s = \sqrt{(-1)}\omega$, $\omega_k = 1/\sqrt{LC_a}$ is the angular frequency of the system, $\zeta = R/(2L)$ the damping coefficient, $\omega_F = 1/\sqrt{L^F C^F}$ is the angular frequency of the feedback element, and $\zeta_F = R^F/(2L^F)$ is the damping coefficient associated with it. With $s^2 + 2s\omega_k\zeta + \omega^2 = 1/H(s)$, $s^2 + 2s\omega_F\zeta + \omega_F^2 = G(s)$ and an output voltage $V_{\rm out}(s) = q/C_T$, where C_T is the effective capacitance at the output, we can write

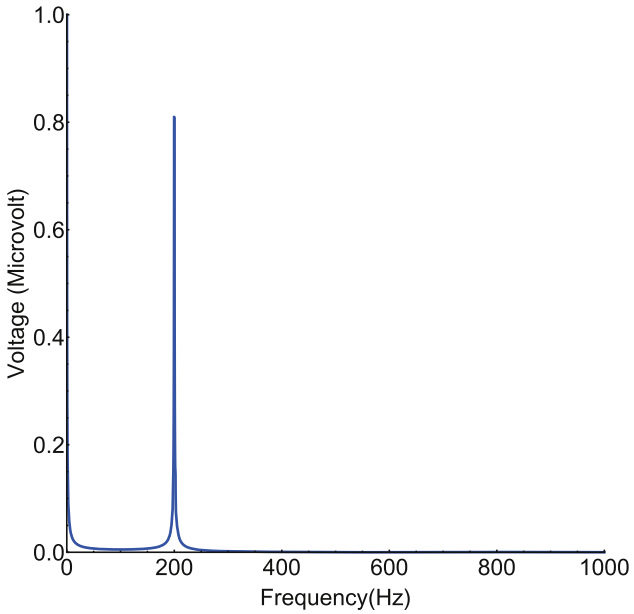

(a)

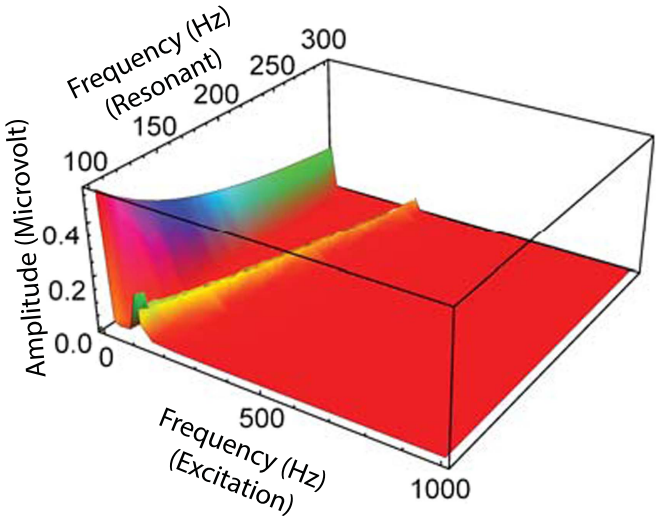

(b)

Figure 5. Mode enhancement under feedback. (a) If an excitation signal arising as a consequence of thermodynamic fluctuation at a frequency of 200 Hz is applied to a crystal having a second order impulse response defined by the thermodynamic fluctuations, the output response shows a dominant mode at 200 Hz in the frequency domain. (b) Secondary modes having relatively high amplitudes are generated when the excitation frequency is continuously varied from 100 to 300 Hz. These modes tend towards singularities as the excitation frequency matches the resonant modes leading to signal amplification, which can be higher in comparison to the Johnson noise by orders of magnitude.

$$V_{\rm out}(s) = \frac{H(s)}{1 - G(s)H(s)} V_{\rm in}(s) = \aleph(s)\, V_{\rm in}(s), \tag{22}$$

with $\aleph(s)$ being the impulse response of the system, leading to an output signal $V_{\rm out}(s)$ that is fed back into the system (figure 4(d)). The function $\aleph(s)$ comprises a number of poles centered about the resonant frequencies. For a general system consisting of a number of resonant frequencies, say ω_k, where $k = 1, \ldots, N$, we can write,

$$V_{\rm out}(s) = \prod_{k=1}^{n} \frac{1}{(s - \omega_k)} V_{\rm in}(s). \tag{23}$$

The response of the system around a single mode at 200 Hz is illustrated in figure 4(c) and it shows a peak. For simplicity, we consider a second-order response of the system having a resonant mode and damping—the net response can be written by equating $V_{\rm in}(s)$ with $V_{\rm out}(s)$ in equation (16).

$$V_{\text{out}}(s) = \frac{\omega_k \alpha}{(s^2 + 2s\omega_k\zeta + \omega^2)} \times \left[\frac{1}{s} - \frac{\beta}{s} + \frac{\chi}{2\sqrt{\xi}} e^{s^2/4\xi}\sqrt{\pi}\ \text{erfc}\left[\frac{s}{2\sqrt{\xi}}\right]\right]. \quad (24)$$

The resultant voltage expressed by equation (24) expresses the response of interaction of an input voltage generated as a consequence of thermodynamic fluctuations to the macroscopic parameters of the dielectric material defined by its transfer function leading to an output voltage. It can be considered as a mathematical expression of the fluctuation dissipation theorem applied to a dielectric material, which underscores the importance of selective mode enhancement under thermodynamic fluctuations. For example, when the input system excites a dielectric material at 200 Hz, the resonant peak is generated at the output as illustrated in figure 5(a). When the system is excited over a range of frequencies from 100 to 200 Hz, a range of peaks are generated as illustrated in figures 5(b). The magnitude of the voltage generated tends towards high values in comparison to the Johnson noise by orders of magnitude. An important conclusion is that unlike Johnson noise —characterized by a uniform spectral density dependent on temperature—bandwidth and resistance, here, the output noise is determined by microscopic as well as macroscopic variables and shows strong frequency dependence.

Although our current understanding of dielectric breakdown incorporates dependence of dielectric strength on intrinsic electrical properties, geometry and temperature [22, 23], the exact role of thermodynamic fluctuations which can generate additional electromagnetic noise under the modulation of dielectric constant has not been reported in the literature so far. However, noise induction in some systems is known to trigger phase transitions associated with changes in the order parameter, leading to symmetry breaking of the system [24]. Under high temperature conditions, the process of electrical breakdown occurs over short-time intervals of the order of a few nanoseconds. Such a regenerative process comes with the generation of free charges as an electrically conductive path is formed between electrodes. This process, in turn, leads to the discharge of conducting species, which can be analyzed within the framework of our study, potentially leading to new insights on the role of specific frequency bands that can get amplified until breakdown occurs.

These considerations are not only important from the perspective of designing insulating materials for high-voltage engineering, but also for the high temperature semiconductor devices where oxide layers work as the insulating barrier between conducting channels. The physical models used to understand thermal runaway resulting in explosion in lithium-ion batteries make extensive use of heat equations [25] which do not incorporate nonequilibrium thermodynamic fluctuations. In such batteries, a dielectric material made of porous polymer separates the anode and cathode electrodes [26, 27]. Structural asymmetries and associated signals in such systems can generate high frequency signals, which in turn can enhance the existing current under positive feedback. This positive feedback can lead to dielectric breakdown and thermal runaway if the frequencies are in the microwave range. Microwave heating and the associated thermal runaway have been extensively investigated [28–31]. The role of thermal runaway in structural failure has been analyzed in viscoelastic materials [32].

5. Conclusion

Thermodynamic fluctuations in a dielectric solid produce effective shifts in the charge cloud around the nuclei of atoms which lead to an effective change in its atomic radius. This results in the generation and propagation of Gaussian pulses of energy creating a similar change in the effective length of the charge cloud around the nuclei, thereby leading to a change in the dielectric constant. Consequently, the modulation of the dielectric constant under thermodynamic fluctuations is an additional source of noise. The magnitude of this induced noise reduces with an increase in frequency in an asymptotic manner, although, around each of the frequency components, the noise shows a Gaussian profile in the time domain. Under the conditions of structural and electrodynamic inhomogeneity, some of the specific frequency modes can get enhanced leading to high-voltage generation under a regenerative effect, which can be estimated using a new formulation of the fluctuation dissipation theorem. The analytical results are highly relevant to the field of design and manufacturing of electronic devices operating at high temperatures where thermodynamic fluctuations play an important role in determining the overall physical behavior. A distinct analysis of noise level in thin films of silicon dioxide and Hafnium dioxide under high temperature might be of additional interest for the CMOS industry.

ORCID iDs

Dhiraj Sinha https://orcid.org/0000-0003-3589-1862
Roland Bouffanais https://orcid.org/0000-0002-2507-4642

References

[1] Nyquist H 1928 *Phys. Rev.* **32** 110
[2] Johnson J B 1928 *Phys. Rev.* **32** 97
[3] Schottky W 1918 *Ann. Phys., Lpz.* **57** 541
[4] Johnson J B 1925 *Phys. Rev.* **26** 71
[5] Davenport W B and Root W L 1958 *Random Signals and Noise* (New York: McGraw-Hill)
[6] Weaver R L and Lobkis O I 2001 *Phys. Rev. Lett.* **87** 134301
[7] Sarpeshkar R, Delbruck T and Mead C A 1993 *IEEE Circuits Devices Mag.* **9** 23
[8] Sinha D and Huang S Y 2016 *J. Appl. Phys.* **120** 074101
[9] Peercy H 2000 *Nature* **406** 1023
[10] Kingon C, Maria A I and Streiffer S K 2002 *Nature* **406** 1032
[11] Campbell C 2012 *Surface Acoustic Wave Devices and Their Signal Processing Applications* (Amsterdam: Elsevier)
[12] Knight H 2003 *Nature* **424** 847
[13] Böttcher C J F, van Belle O C, Bordewijk P and Rip A 1978 *Theory of Electric Polarization* vol 2 (Amsterdam: Elsevier)
[14] Dekker A J 1959 *Electrical Engineering Materials* vol 969 (New York: Prentice-Hall)
[15] Pierson H O 2012 *Handbook of Carbon, Graphite, Diamonds and Fullerenes: Processing, Properties and Applications* (Norwich, NY: William Andrew)
[16] Saito R, Dresselhaus G and Dresselhaus M S 1998 *Physical Properties of Carbon Nanotubes* (Singapore: World Scientific)
[17] Wooten E L *et al* 2000 *IEEE J. Sel. Top. Quantum Electron.* **6** 69
[18] Mansingh A and Dhar A 1985 *J. Phys. D: Appl. Phys.* **18** 2059
[19] Guha P K, Ali S Z, Lee C, Udrea F, Milne W, Iwaki T, Covington J A and Gardner J 2007 *Sensors Actuators* B **127** 260
[20] Zhang B and Kahrizi M 2007 *IEEE Sens. J.* **7** 586
[21] Ogata K and Yang Y 1970 *Modern Control Engineering* (Englewood Cliffs, NJ: Prentice-Hall)
[22] O'Dwyer J J 1973 *The Theory of Electrical Conduction and Breakdown in Solid Dielectrics* (Oxford: Clarendon)
[23] Kunhardt E E and Luessen L H 2013 *Electrical Breakdown and Discharges in Gases: Part A Fundamental Processes and Breakdown* vol 89 (New York: Springer Science & Business Media)
[24] Van den Broeck C, Parrondo J and Toral R 1994 *Phys. Rev. Lett.* **73** 3395
[25] Wang Q, Ping P, Zhao X, Chu G, Sun J and Chen C 2012 *J. Power Sources* **208** 210
[26] Yoshio M, Brodd R J and Kozawa A 2009 *Lithium-Ion Batteries* vol 1 (Berlin: Springer)
[27] Meyer W H 1998 *Adv. Mater.* **10** 439
[28] Wu X, Thomas J Jr and Davis W A 2002 *J. Appl. Phys.* **92** 3374
[29] Vriezinga C, Sanchez-Pedreno S and Grasman J 2002 *Appl. Math. Modelling* **26** 1029
[30] Kriegsmann G A 1992 *J. Appl. Phys.* **71** 1960
[31] Moriwaki S, Machida M, Tatsumoto H, Kuga M and Ogura T 2006 *J. Anal. Appl. Pyrolysis* **76** 238
[32] Braeck S and Podladchikov Y 2007 *Phys. Rev. Lett.* **98** 095504